A magnesium ion core at the heart of a ribozyme domain

Jamie H. Cate, Raven L. Hanna and Jennifer A. Doudna

Large ribozymes require divalent metal ions to fold. We show here that the tertiary structure of the *Tetrahymena* group I intron P4-P6 domain nucleates around a magnesium ion core. In the domain crystal structure, five magnesium ions bind in a three-helix junction at the centre of the molecule. Single atom changes in any one of four magnesium sites in this three-helix junction destroy folding of the entire 160-nucleotide P4-P6 domain. The magnesium ion core may be the RNA counterpart to the protein hydrophobic core, burying parts of the RNA molecule in the native structure.

In many proteins, buried hydrophobic residues form a core around which the native structure folds[1]. Equivalent structural principles for RNA tertiary folding are unknown. The active structures of large RNAs are thought to contain domains of stacked helices that pack together through tertiary contacts[2,3]. Magnesium ions play fundamental roles in the formation and stability of these structures[4].

In the *Tetrahymena* group I self-splicing intron, as in tRNA[5], RNA folding is hierarchical: base pairing precedes formation of tertiary structure[6,7]. Transfer RNAs and the hammerhead ribozyme can adopt their native structure in the presence of either monovalent or divalent cations[5,8–10]. Group I introns and other large ribozymes, however, require divalent metal ions for tertiary folding[4,11].

The *Tetrahymena* intron contains two large domains[2] (base-paired (P) regions P4-P6 and P1-P2.1/P3-P9; Fig. 1*a*)[7,11,12] that fold sequentially in a magnesium-dependent manner. The P4-P6 domain (Fig. 1 *a*,*b*) folds before the rest of the ribozyme[7,13] and forms its native structure when synthesized as a separate RNA[14]. Within the intact intron, as well as in the P4-P6 domain alone, helices P5a–P5c (P5abc; Fig. 1*c*) require the lowest concentration of Mg^{2+} to fold[11,14]. In fact, the P5abc three-helix junction is itself a stable subdomain[14].

A striking feature of the P4-P6 domain crystal structure[15] is the clustering of divalent metal ions in the P5abc subdomain (Fig. 1*b*). Within the P4-P6 molecule, the subdomain is the most complex region of tertiary folding. The subdomain three-helix junction buttresses the A-rich bulge, an adenosine-rich corkscrew that forms key tertiary interactions bridging the helical halves of the P4-P6 RNA (Fig. 1*b*)[15]. Together with the above biochemical data, the structure suggests that specific magnesium ions may organize the three-helix junction and drive the normal folding pathway of the P4-P6 domain and, ultimately, of the entire ribozyme. Rather than folding around a hydrophobic core, this large RNA may fold around a metal ion core.

Manganese substitution in P4-P6 domain crystals

To prove the identity of magnesium ions in the P4-P6 domain, crystals were transferred to a solution containing no magnesium, 5 mM manganese chloride and 4 mM spermine. X-ray diffraction data measured from a manganese-soaked crystal were used to calculate an anomalous difference Fourier electron density map, revealing 14 peaks of 7σ or more above the mean (Fig. 1*b*). Six peaks appear at identical positions in each of the two molecules in the asymmetric unit of the crystal. One may be due to cobalt hexammine bound in the major groove of P5b[16] (Fig. 1*b*,*c*). The remaining five peaks occur at precisely the locations of the magnesium ions bound in the three-helix junction and the A-rich bulge, as modelled in the original structure (Fig. 2*a*).

These five metal ions bridge noncontiguous nucleotides to form a structural core that buries parts of the RNA backbone in this region[14,15]. Each of the ions binds to the RNA through at least one direct (inner-sphere) coordination. Two metals are positioned above and below the plane of the A-rich bulge corkscrew[15], each directly coordinated by three phosphate oxygens (Fig. 2*b*). A third metal, ringed by phosphates from helix P5c, binds to the carbonyl oxygen of G188 above the corkscrew (Fig. 2*c*). Two sheared G–A base pairs that top the P5b helix close to the junction coordinate a fourth metal through the N7 and O6 functional groups of the adjacent guanosine bases (Fig. 2*d*). Finally, the adenosine platform[17] in the loop of L5c binds to a fifth metal through the pro-R_p phosphate oxygen of A171 (Fig. 2*e*).

Dept. of Molecular Biophysics and Biochemistry, Yale University, New Haven, Connecticut 06520, USA.

Correspondence should be addressed to J.A.D. *email: doudna@csb.yale.edu*

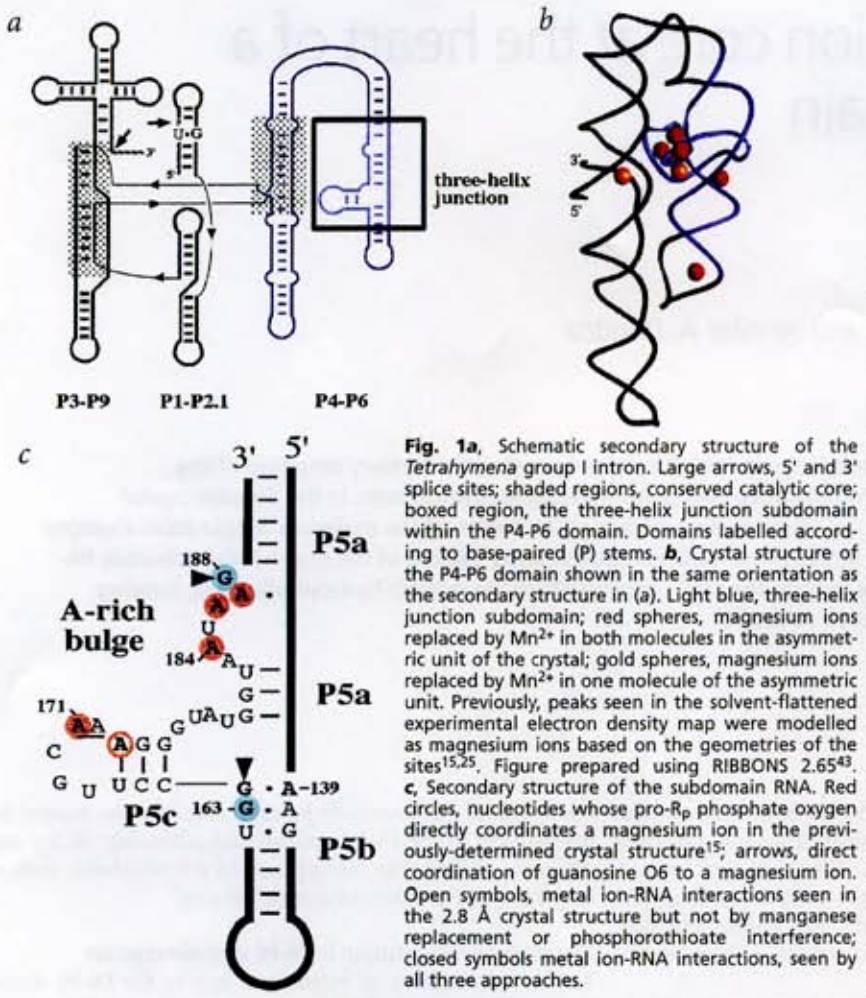

Fig. 1a, Schematic secondary structure of the *Tetrahymena* group I intron. Large arrows, 5' and 3' splice sites; shaded regions, conserved catalytic core; boxed region, the three-helix junction subdomain within the P4-P6 domain. Domains labelled according to base-paired (P) stems. ***b***, Crystal structure of the P4-P6 domain shown in the same orientation as the secondary structure in (*a*). Light blue, three-helix junction subdomain; red spheres, magnesium ions replaced by Mn^{2+} in both molecules in the asymmetric unit of the crystal; gold spheres, magnesium ions replaced by Mn^{2+} in one molecule of the asymmetric unit. Previously, peaks seen in the solvent-flattened experimental electron density map were modelled as magnesium ions based on the geometries of the sites[15,25]. Figure prepared using RIBBONS 2.65[43]. **c**, Secondary structure of the subdomain RNA. Red circles, nucleotides whose pro-R_p phosphate oxygen directly coordinates a magnesium ion in the previously-determined crystal structure[15]; arrows, direct coordination of guanosine O6 to a magnesium ion. Open symbols, metal ion-RNA interactions seen in the 2.8 Å crystal structure but not by manganese replacement or phosphorothioate interference; closed symbols metal ion-RNA interactions, seen by all three approaches.

Disruption of folding by phosphorothioates

If the identified divalent metal ions play active roles in P4-P6 domain folding, disruption of the magnesium binding sites should prevent the RNA from adopting its native structure. Since the pro-R_p phosphate oxygens of four adenosines directly coordinate divalent ions (A171, A184, A186 and A187; Fig. 1*c* and Fig. 2*b*,*e*), the functional importance of at least three of the five metals could be tested by phosphorothioate substitution interference[18]. Sulphur atoms, readily incorporated into RNA as R_p phosphorothioates, coordinate magnesium ions 30,000 times more weakly than do oxygen atoms[19].

Two molecules were tested for magnesium-dependent folding: the 160-nucleotide P4-P6 domain and a 56-nucleotide RNA consisting of the subdomain three-helix junction[14] (Fig. 1). Mutants of the two molecules (A186U) served as controls for unfolding[20]. The P4-P6 domain and subdomain RNAs require magnesium ions to fold, as shown by mobility in nondenaturing polyacrylamide gels (Fig. 3*a*) and by Fe-EDTA footprinting[14] (E. Doherty and J.A.D., unpublished data). For the phosphorothioate substitution experiments, each RNA was transcribed in four separate reactions, each containing one of the α-phosphorothioate nucleotides (A, C, G or U). The concentrations of nucleotides were adjusted such that, on average, one R_p phosphorothioate substitution occurred per RNA molecule[18]. Significantly, relative to the C, G or U α-phosphorothioate containing samples, more of the adenosine α-phosphorothioate containing RNA failed to fold (Fig. 3*a*).

The folded and unfolded RNAs in each sample were isolated, and sulphur substitutions that prevented folding were mapped by iodine/ethanol cleavage of the RNA backbone[21]. Sequencing gels of the iodine-cleaved RNAs revealed seven positions at which a single phosphorothioate substitution destroys RNA tertiary structure (Fig. 3*b*). These positions are identical in the P4-P6 domain and the P5abc subdomain RNAs. Apart from one substitution that disrupts an RNA–RNA hydrogen bond (A139, manuscript in preparation), all the sites involve coordination to four magnesium ions in the subdomain. Sulphur replacement at any one of the pro-R_p phosphate oxygens directly coordinating Mg^{2+} ions (A171, A184, A186 or A187) prevents RNA folding. At two other sites (G163 and G188), phosphorothioate substitution may block folding by weakening hydrogen bonds to metal-coordinated water molecules or by causing a steric clash[22,23] (Fig. 2*b*,*d*).

Modes of magnesium binding

Magnesium and manganese ion binding sites in the P4-P6 domain can be compared to those in tRNA and the hammerhead ribozyme, the only other non-duplex RNAs whose crystal structures are currently known. In contrast to our results, manganese ions usually did not bind to tRNA and the hammerhead in the same way as magnesium ions[9,10,24,25]. Direct coordination of magnesium ions to base functional groups was also not observed in these RNAs. Based on native electron density maps and lanthanide ion replacement, three magnesium binding sites in tRNA were identified that involve direct coordination of one or two phosphate oxygens to the ion[24,25]. One such site was found in the hammerhead ribozyme[10]. The differences in number and specificity of magnesium coordination sites in tRNA and the hammerhead ribozyme compared to those in the P4-P6 domain may reflect both the design of the manganese replacement experiments in each case and fundamental structural differences between these RNAs. We suspect that at the high spermine concentration used in our experiments (4 mM), spermine competed for weak magnesium ion binding sites, since only seven peaks per molecule appear in the anomalous difference Fourier map. For example, three fully hydrated magnesium ions seen in experimental electron density maps to bind the P4-P6 domain through outer sphere coordination are not replaced by Mn^{2+} in the anomalous difference Fourier experiment. Thus, only the most specific divalent metal binding sites were bound by manganese ions in the P4-P6 domain crystals.

A metal ion core in the *Tetrahymena* group I intron

Unlike tRNA and the hammerhead ribozyme, the P4-P6 domain involves extensive helical packing that creates a solvent inaccessible interior[14,15]. Magnesium ions play a different and more specific role in the tertiary folding of the P4-P6 domain by burying phosphate oxygens exposed in the unfolded state. Within the native

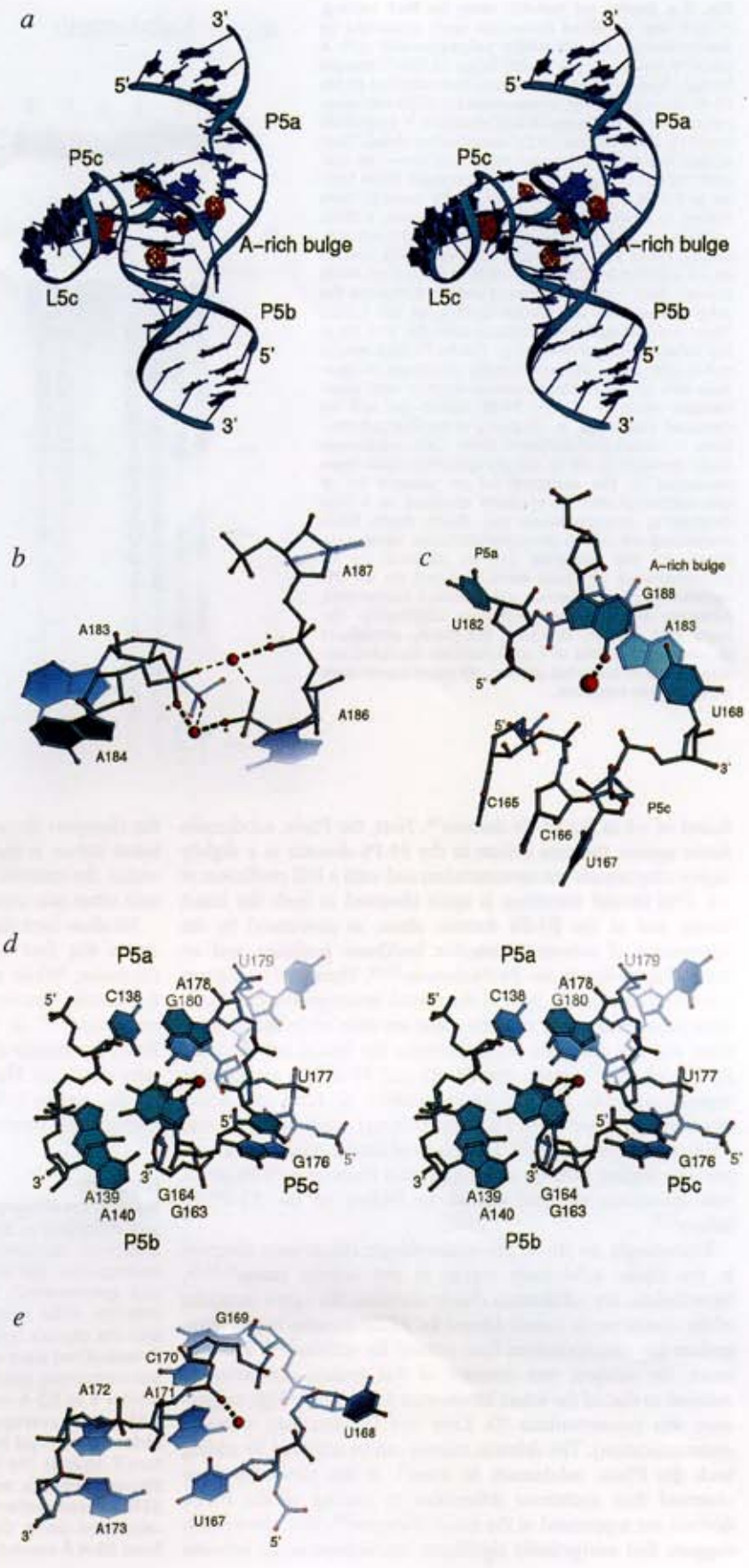

Fig. 2 The magnesium ion core of the P4-P6 domain. ***a***, Stereo view of the three-helix junction (blue) superimposed on the anomalous difference Fourier electron density map (red) contoured at 5.7σ above the mean. The five difference density peaks correspond exactly to the locations of the five magnesium ions positioned in the 2.8 Å resolution structure[15]. ***b***, Two magnesium ions (large red spheres) each directly coordinate to three phosphate oxygens in the A-rich bulge. Thick dashed lines are to oxygens whose substitution with sulphur destroys folding of the subdomain and the entire P4-P6 domain (Fig. 3). The pro-R_p oxygen of G188 probably coordinates a metal-bound water. ***c***, G188 coordinates a magnesium ion directly through its carbonyl oxygen; phosphates ring this binding pocket at the top of the three-helix junction. ***d***, Two tandem sheared G–A base pairs at the bottom of the junction, which coordinate a magnesium ion through guanosine O6 and N7 groups. G163 may coordinate an outer-sphere water through its pro-R_p oxygen (stereo view). ***e***, A fifth magnesium ion binds below A171 in the L5c A-platform. Figure prepared using RIBBONS 2.65[43] and MIDASPlus, a program developed at the Computer Graphics Laboratory, University of California, San Francisco (supported by the NIH).

structure, many phosphate oxygens in the P5abc subdomain are inaccessible to solvent (Fig. 4). These phosphate oxygens mainly involve inner-sphere or outer-sphere coordination to magnesium ions, forming a highly charged core not unlike a hydrated salt. This ionic environment, while chemically distinct from the hydrophobic core of proteins, likewise provides a large contribution to tertiary folding. In proteins, a well-packed hydrophobic core is favoured over buried salt bridges[26], probably since electrostatic interactions in the folded state do not overcome the large cost of side chain desolvation[27,28]. In the P4-P6 domain, magnesium ion binding involves a large number of ionic and hydrogen bonds, which could overcome the cost of phosphate and magnesium desolvation.

Divalent metal ion binding is the driving factor in forming the tertiary structure of the *Tetrahymena* ribozyme. In the absence of Mg^{2+}, the intron forms most of its secondary structure but little, if any, of its tertiary structure[6,11,29]. At least three cooperative folding transitions occur as a function of magnesium ion concentration on the intron folding pathway. Specific positions in the P5abc subdomain backbone become protected from free radical cleavage at the lowest concentration of magnesium ion, both in the intact intron and in the P4-P6 domain alone[11,14]. The cooperativity of P5abc subdomain folding has a Hill coef-

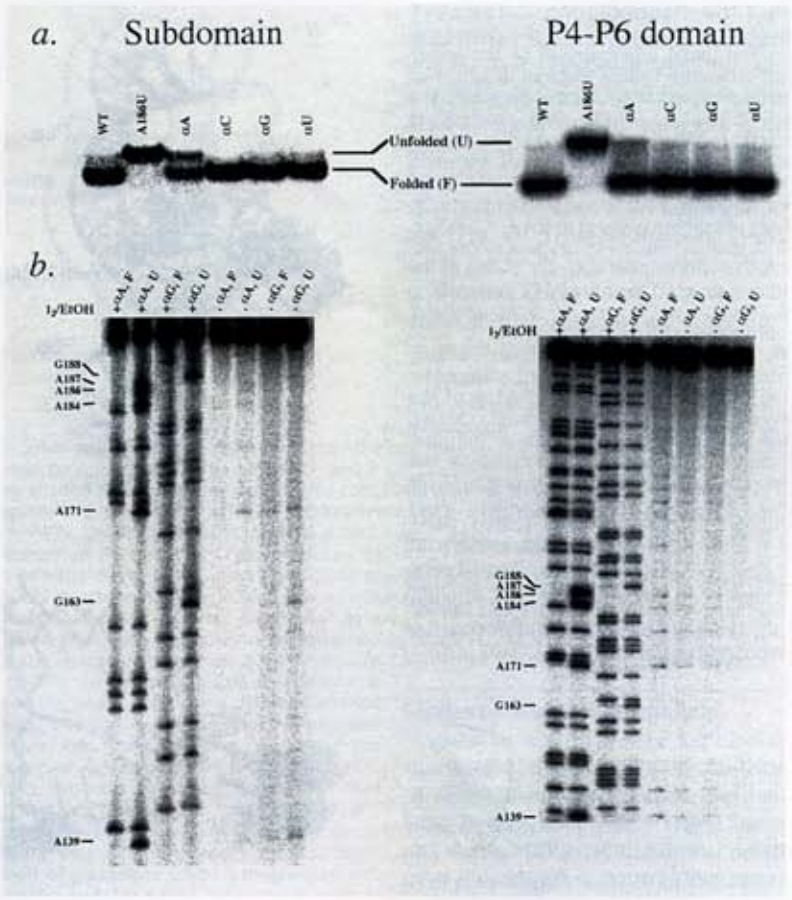

Fig. 3 ***a***, Native gel mobility assay for RNA folding. Folded and unfolded molecules were separated by electrophoresis on 8% native polyacrylamide gels. A point mutation in the A-rich bulge (A186U) disrupts tertiary folding of both the subdomain and the entire P4-P6 domain even at a concentration of 50 mM magnesium ion[20], while secondary structure is essentially intact (E. Doherty and J.A.D., unpublished data). Thus, A186U mutants of the two molecules served as controls for unfolding. Left panel, subdomain RNAs folded in 5 mM $MgCl_2$; right panel, P4-P6 domain RNAs folded in 2 mM $MgCl_2$. WT, wild type RNA; A186U, unfolded mutant RNA; αN, phosphorothioate-containing RNAs. We consistently observed ~30% unfolded αA subdomain RNA and ~10% unfolded αA P4-P6 domain RNA, while the percent unfolded RNA for the other αN samples was similar to that for WT (<5%). These percentages are consistent with the 5/17 A's in the subdomain and 5/44 A's in the P4-P6 RNA whose pro-R_p phosphate oxygens directly coordinate magnesium ions in the crystal structure. Species with intermediate mobility in the P4-P6 native gel will be discussed elsewhere. ***b***, Mapping of sulphur substitutions in folded and unfolded RNAs. Left, subdomain RNAs containing αA or αG phosphorothioates were incubated in the presence (+) or absence (-) of iodine/ethanol and the products analyzed on a 10% denaturing polyacrylamide gel. Right, P4-P6 RNAs containing αA or αG phosphorothioates were incubated in the presence (+) or absence (-) of iodine/ethanol; products were analyzed on an 8% denaturing polyacrylamide gel. Labelled nucleotides, positions where phosphorothioate substitution disrupts RNA tertiary structure. No pro-R_p phosphate oxygen substitutions of C or U residues disrupted tertiary structure (data not shown). All experiments were performed in triplicate.

ficient of ~3 in the P4-P6 domain[14]. Next, the P5abc subdomain docks against the core helices in the P4-P6 domain at a slightly higher magnesium ion concentration and with a Hill coefficient of ~4. This second transition is again observed in both the intact intron and in the P4-P6 domain alone, as monitored by the appearance of solvent-inaccessible backbone positions and an internal cross-link in the P4-P6 domain[13,14]. These two transitions can be rationalized in light of the crystal structure: the first backbone protections occur near the metal ion core, while later protections and the cross-link occur between the helical halves of the P4-P6 domain[15]. Finally, the P8, P3 and P7 helices and joining regions assemble on the P4-P6 scaffold to form the active ribozyme structure[12,13,30]. This third folding transition occurs with a Hill coefficient of ~8[13,30]. The results of kinetic experiments support this folding pathway and suggest that P5abc and P4-P6 structure formation are fast relative to folding of the P3-P7-P8 helices[7,13].

Interestingly, no strong phosphorothioate effects were observed in the P5abc subdomain region in any activity assays[18,31,32]. Nonetheless, the subdomain clearly stabilizes the active structure of the ribozyme: an intron deleted for P5abc requires higher magnesium ion concentrations than normal for activity[33,34]. Furthermore, the catalytic rate constant of this mutant can never be restored to that of the intact intron even at extremely high magnesium ion concentrations (D. Knitt and D. Herschlag, personal communication). The deletion mutant can be activated by adding back the P5abc subdomain in *trans*[35]. It has previously been observed that mutations deleterious to folding of the P4-P6 domain are suppressed in the intact ribozyme[34]. This observation suggests that energetically significant interactions occur between the ribozyme domains, and that folding of these domains in the intact intron is highly coupled. In addition to domain contacts within the catalytic core, the P4-P6 domain is known to interact with other non-conserved elements of the intron[34,36,37].

We show here that the metal ion core in the P5abc subdomain drives the first two folding transitions of the *Tetrahymena* ribozyme. While metal-dependent folding occurs in proteins, the motifs involved are small and often require just a single metal ion[38,39]. In the case of the P4-P6 domain, a 52,000 M_r RNA, five metals all play indispensable roles in forming the tertiary structure. Thus, the metal ion core may provide a scaffold in the native structures of large RNAs, analogous to the hydrophobic core in proteins.

Methods

X-ray crystallography. Crystals of the P4-P6 domain were grown and stabilized as described[15,16]. Crystals were then transferred to a solution containing 25% 2-methyl-2,4 pentanediol (MPD), 10% isopropanol, 100 mM potassium cacodylate pH 6.0, 50 mM KCl, 4 mM spermine-HCl, 5 mM $MgCl_2$ and 0.1 mM cobalt hexammine chloride. After 15 min, the $MgCl_2$ was replaced with 5 mM $MnCl_2$ and the crystals left for three days. X-ray diffraction data (20–3.5 Å resolution) were measured at 105 K from a crystal soaked in the Mn-containing solution (rotating anode source, Cu Kα radiation; $I/\sigma(I)$ = 5 at 3.5 Å resolution, completeness = 99% to 3.5 Å, R_{sym} = 9.6% on I, average redundancy = 4). A new P4-P6 model was obtained by rigid body refinement of the 2.8 Å resolution structure[16] against the Mn^{2+} soaked crystal diffraction amplitudes[40]. Phases from this model were refined by solvent flattening with 65% solvent content[41]. Anomalous difference Fourier maps were calculated using the refined phases and diffraction amplitudes from 20–4 Å resolution.

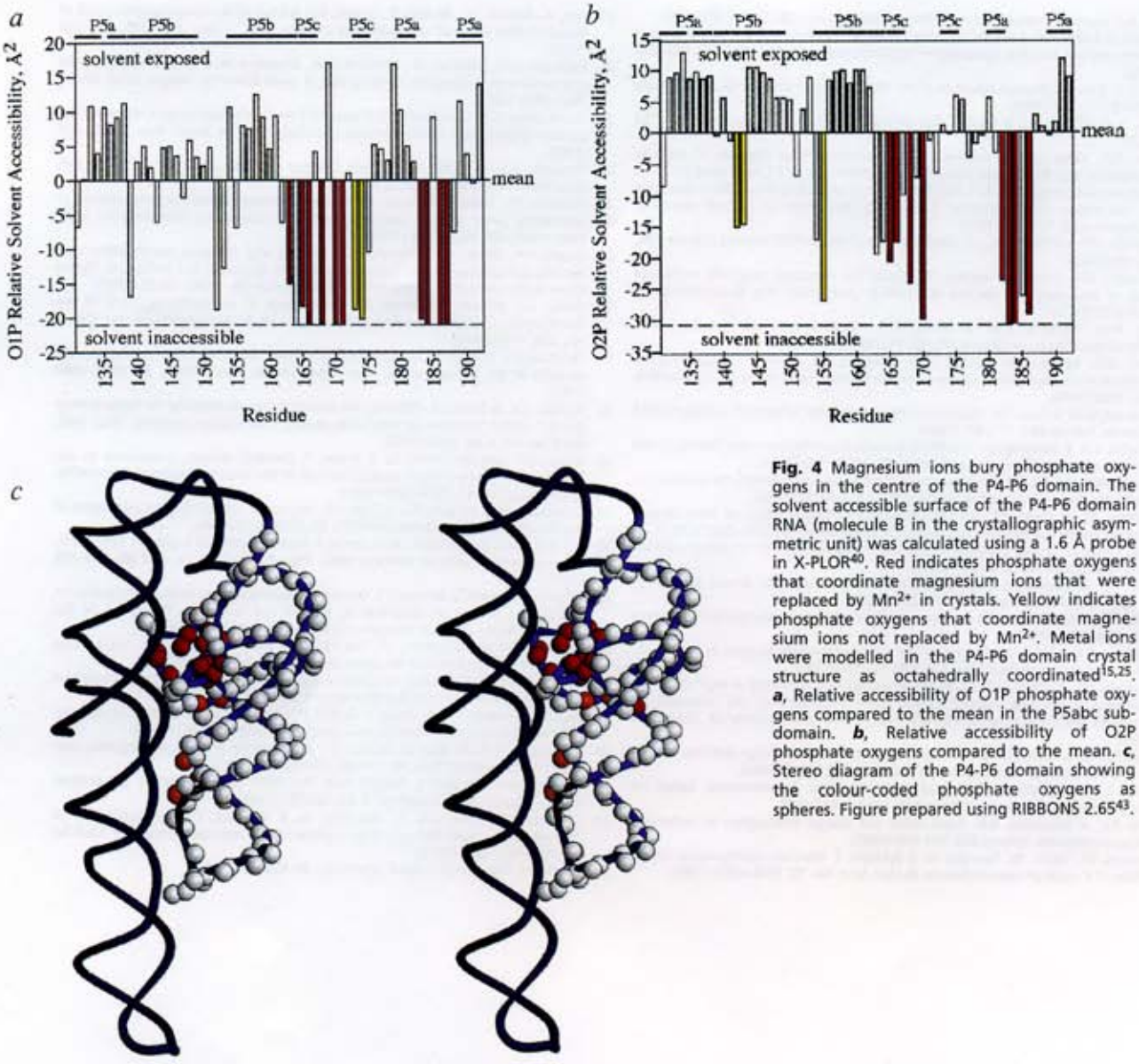

Fig. 4 Magnesium ions bury phosphate oxygens in the centre of the P4-P6 domain. The solvent accessible surface of the P4-P6 domain RNA (molecule B in the crystallographic asymmetric unit) was calculated using a 1.6 Å probe in X-PLOR[40]. Red indicates phosphate oxygens that coordinate magnesium ions that were replaced by Mn^{2+} in crystals. Yellow indicates phosphate oxygens that coordinate magnesium ions not replaced by Mn^{2+}. Metal ions were modelled in the P4-P6 domain crystal structure as octahedrally coordinated[15,25]. ***a***, Relative accessibility of O1P phosphate oxygens compared to the mean in the P5abc subdomain. ***b***, Relative accessibility of O2P phosphate oxygens compared to the mean. ***c***, Stereo diagram of the P4-P6 domain showing the colour-coded phosphate oxygens as spheres. Figure prepared using RIBBONS 2.65[43].

Phosphorothioate substitution interference. P4-P6 RNA was transcribed *in vitro* as described[42]. Mutant A186U P4-P6 RNA and subdomain RNAs were transcribed from PCR-amplified plasmid templates. Four pools of RNA molecules were prepared by *in vitro* transcription reactions doped individually with A, C, G or U α-phosphorothioate nucleotides. Concentrations of nucleotides and the phosphorothioate analog were adjusted such that each molecule contained approximately one phosphorothioate substitution[18]. Transcripts were purified by denaturing polyacrylamide gel electrophoresis, 5'-dephosphorylated with calf intestinal phosphatase, and 5'-end-labelled with ^{32}P using T4 polynucleotide kinase. After phenol/chloroform extraction and ethanol precipitation, the subdomain RNAs were incubated in 100mM Tris-HEPES pH 7.5, 10% glycerol and 5 mM $MgCl_2$ for three minutes at 80 °C and allowed to cool to room temperature; the P4-P6 domain RNAs were incubated in a similar buffer containing 2 mM $MgCl_2$ at 65 °C for five minutes. Folded and unfolded RNAs were separated on nondenaturing 8% polyacrylamide gels containing 100 mM Tris-HEPES pH 7.5, 0.1 mM EDTA and 5 mM $MgCl_2$ for the subdomain, or 2 mM $MgCl_2$ for P4-P6. The eluted RNA samples were phenol/chloroform extracted, ethanol precipitated, resuspended in formamide loading buffer (FLB, 45% formamide, 10 mM Tris pH 8.0 and 1.0 mM EDTA) and purified on denaturing 10% polyacrylamide gels. The radioactivity of each sample was normalized prior to iodine/ethanol sequencing[21]. Each RNA sample was divided in half and incubated briefly at room temperature in FLB with or without iodine/ethanol. The resulting products were resolved by denaturing polyacrylamide gel electrophoresis. Gels were scanned with a Fuji phosphorimager and the resulting images visualized with MacBas 2.0.

Acknowledgements

We thank Kaihong Zhou for excellent technical assistance, Scott Strobel for providing the A186U *Tetrahymena* intron mutant plasmid, Carl Correll, Liz Doherty, Fred Richards and Paul Sigler for helpful discussions, and Virginia Rath, Lynne Regan and Tom Steitz for comments on the manuscript. J.A.D. is a Lucille Markey Scholar in Biomedical Science, a Donaghue Foundation Young Investigator, a Beckman Foundation Young Investigator, a Searle Scholar and a Fellow of the David and Lucile Packard Foundation. This work was supported by the Lucille Markey Charitable Trust, the Beckman Foundation, the Searle Scholars Program and the NIH.

Received 24 February 1997; Accepted 30 May 1997.

1. Dill, K.A. Dominant forces in protein folding. *Biochemistry* **29**, 7133–7155 (1990).
2. Michel, F. & Westhof, E. Modelling of the three-dimensional architecture of group I catalytic introns based on comparative sequence analysis. *J. Mol. Biol.* **216**, 585–610 (1990).
3. Loria, A. & Pan, T. Domain structure of the ribozyme from eubacterial ribonuclease P. *RNA* **2**, 551–563 (1996).
4. Pyle, A.M. Ribozymes: a distinct class of metalloenzymes. *Science* **261**, 709–714 (1993).
5. Cole, P.E., Yang, S.K. & Crothers, D.M. Conformational changes of transfer ribonnucleic acid: Equilibrium phase diagrams *Biochemistry* **11**, 4358–4368 (1972).
6. Banerjee, A.R., Jaeger, J.A. & Turner, D.H. Thermal unfolding of a group I ribozyme: the low-temperature transition is primarily disruption of tertiary structure. *Biochemistry* **32**, 153–163 (1993).
7. Zarrinkar, P.P. & Williamson, J.R. Kinetic intermediates in RNA folding. *Science* **265**, 918–924 (1994).
8. Robillard, G.T., Tarr, C.E., Vosman, F. & Reid, B.R. A nuclear magnetic resonance study of secondary and tertiary structure in yeast tRNA Phe. *Biochemistry* **16**, 5261–5273 (1977).
9. Pley, H.W., Flaherty, K.M. & McKay, D.B. Three-dimensional structure of a hammerhead ribozyme. *Nature* **372**, 68–74 (1994).
10. Scott, W.G., Murray, J.B., Arnold, J.R.P., Stoddard, B.L. & Klug, A. Capturing the structure of a catalytic RNA intermediate: the hammerhead ribozyme. *Science* **274**, 2065–2069 (1996).
11. Celander, D.W. & Cech, T.R. Visualizing the higher order folding of a catalytic RNA molecule. *Science* **251**, 401–407 (1991).
12. Doherty, E.A. & Doudna, J.A. The P4-P6 domain directs higher order folding of the *Tetrahymena* ribozyme core. *Biochemistry* **36**, 3159–3169 (1997).
13. Downs, W.D. & Cech, T.R. Kinetic pathway for folding of the *Tetrahymena* ribozyme revealed by three UV-inducible crosslinks. *RNA* **2**, 718–732 (1996).
14. Murphy, F.L. & Cech, T.R. An independently folding domain of RNA tertiary structure within the *Tetrahymena* ribozyme. *Biochemistry* **32**, 5291–5300 (1993).
15. Cate, J.H. *et al.* Crystal structure of a group I ribozyme domain: Principles of RNA packing. *Science* **273**, 1678–1685 (1996).
16. Cate, J.H. & Doudna, J.A. Metal binding sites in the major groove of a large ribozyme domain. *Structure* **4**, 1221–1229 (1996).
17. Cate, J.H. *et al.* RNA tertiary structure mediation by adenosine platforms. *Science* **273**, 1696–1699 (1996).
18. Christian, E.L. & Yarus, M. Analysis of the role of phosphate oxygens in the group I intron from *Tetrahymena*. *J Mol. Biol.* **228**, 743–758 (1992).
19. Pecoraro, V.L., Hermes, J.D. & Cleland, W.W. Stability constants of Mg^{2+} and Cd^{2+} complexes of adenine nucleotides and thionucleotides and rate constants for formation and dissociation of Mg-ATP and Mg-ADP. *Biochemistry* **23**, 5262–5271 (1984).
20. Murphy, F.L. & Cech, T.R. GAAA tetraloop and conserved bulge stabilize tertiary structure of a group I intron domain. *J Mol. Biol.* **236**, 49–63 (1994).
21. Gish, G. & Eckstein, F. DNA and RNA sequence determination based on phosphorothioate chemistry. *Science* **240**, 1520–1522 (1988).
22. Frey, P.A. & Sammons, R.D. Bond order and charge localization in nucleoside phosphorothioates. *Science* **228**, 541–545 (1985).
23. Hinrichs, W., Steifa, M., Saenger, W. & Eckstein, F. Absolute configuration of Rp-uridine 3',5'-cyclic phosphorothioate. *Nucleic Acids Res.* **15**, 4945–4955 (1987).
24. Jack, A., Ladner, J.E., Rhodes, D., Brown, R.S. & Klug, A. A crystallographic study of metal-binding to yeast phenylalanine transfer RNA. *J. Mol. Biol.* **111**, 315–328 (1977).
25. Holbrook, S.R., Sussman, J.L., Warrant, R.W., Church, G.M. & Kim, S.-H. RNA-ligand interactions: (i) magnesium binding sites in yeast tRNAPhe. *Nucleic Acids Res.* **4**, 2811–2820 (1977).
26. Waldburger, C.D., Schildbach, J.F. & Sauer, R.T. Are buried salt bridges important for protein stability and conformational specificity? *Nature Struct. Biol.* **2**, 122–128 (1995).
27. Hendsch, Z.S. & Tidor, B. Do salt bridges stabilize proteins? A continuum electrostatic analysis. *Prot. Sci.* **3**, 211–226 (1994).
28. Hendsch, Z.S., Jonsson, T., Sauer, R.T. & Tidor, B. Protein stabilization by removal of unsatisfied polar groups: computational approaches and experimental tests. *Biochemistry* **35**, 7621–7625 (1996).
29. Jaeger, J.A., Zuker, M. & Turner, D.H. Melting and chemical modification of a cyclized self-splicing group I intron: similarity of structures in 1 M Na+, in 10 mM Mg2+, and in the presence of substrate. *Biochemistry* **29**, 10147–10158 (1990).
30. Wang, J.-F. & Cech, T.R. Metal ion dependence of active-site structure of the *Tetrahymena* ribozyme revealed by site-specific photo-cross-linking. *J. Am. Chem. Soc.* **116**, 4178 (1994).
31. Christian, E.L. & Yarus, M. Metal coordination sites that contribute to structure and catalysis in the group I intron from *Tetrahymena*. *Biochemistry* **32**, 4475–4480 (1993).
32. Strobel, S.A. & Shetty, K. Defining the chemical groups essential for *Tetrahymena* group I intron function by nucleotide analog interference mapping. *Proc. Natl. Acad. Sci. U.S.A.* **94**, 2903 (1997).
33. Joyce, G.F., van der Horst, G. & Inoue, T. Catalytic activity is retained in the *Tetrahymena* group I intron despite removal of the large extension of element P5. *Nucleic Acids Res* **17**, 7879–7889 (1989).
34. Laggerbauer, B., Murphy, F.L. & Cech, T.R. Two major tertiary folding transitions of the *Tetrahymena* catalytic RNA. *EMBO J.* **13**, 2669–2676 (1994).
35. van der Horst, G., Christian, A. & Inoue, T. Reconstitution of a group I intron self-splicing reaction with an activator RNA. *Proc. Natl. Acad. Sci. USA* **88**, 184–188 (1991).
36. Lehnert, V., Jaeger, L., Michel, F. & Westhof, E. New loop-loop tertiary interactions in self-splicing introns of subgroup IC and ID - A complete 3D model of the *Tetrahymena thermophila* ribozyme. *Chem. & Biol.* **3**, 993–1009 (1996).
37. Zarrinkar, P.P. & Williamson, J.R. The P9.1-P9.2 peripheral extension helps guide folding of the *Tetrahymena* ribozyme. *Nucleic Acids Res.* **24**, 854 (1996).
38. Coleman, J.E. Zinc proteins: enzymes, storage proteins, transcription factors and replication proteins. *Annu. Rev. Biochem.* **61**, 897–946 (1992).
39. Wu, L.C., Schulman, B.A., Peng, Z. & Kim, P.S. Disulfide determinants of calcium-induced packing in alpha-lactalbumin. *Biochemistry* **35**, 859–863 (1996).
40. Brünger, A. *X-PLOR Manual, Version 3.1: A System for X-ray Crystallography and NMR* (Yale University Press, New Haven, Connecticut; 1993).
41. Collaborative Computing Project, N.4. The CCP4 suite: programs for protein crystallography. *Acta Crystallogr.*. D **50**, 760–763 (1994).
42. Doudna, J.A., Grosshans, C., Gooding, A. & Kundrot, C.E. Crystallization of ribozymes and small RNA motifs by a sparse matrix approach. *Proc Natl Acad Sci USA* **90**, 7829–7833 (1993).
43. Carson, M. Ribbons 2.0. *J. Appl. Crystallogr.* **24**, 958–961 (1991).